



LAWRENCE
LIVERMORE
NATIONAL
LABORATORY

LLNL-JRNL-741222

COX-2/sEH Dual Inhibitor PTUPB Potentiates the Anti-tumor Efficacy of Cisplatin

F. Wang, H. Zhang, A. Ma, M. Zimmermann, S. H. Hwang, D. Zhu, T. Lin, M. Malfatti, K. Turteltaub, P. Henderson, B. D. Hammock, J. Yuan, R. W. de Vere White, C. Pan

November 6, 2017

Molecular Cancer Therapeutics

Disclaimer

This document was prepared as an account of work sponsored by an agency of the United States government. Neither the United States government nor Lawrence Livermore National Security, LLC, nor any of their employees makes any warranty, expressed or implied, or assumes any legal liability or responsibility for the accuracy, completeness, or usefulness of any information, apparatus, product, or process disclosed, or represents that its use would not infringe privately owned rights. Reference herein to any specific commercial product, process, or service by trade name, trademark, manufacturer, or otherwise does not necessarily constitute or imply its endorsement, recommendation, or favoring by the United States government or Lawrence Livermore National Security, LLC. The views and opinions of authors expressed herein do not necessarily state or reflect those of the United States government or Lawrence Livermore National Security, LLC, and shall not be used for advertising or product endorsement purposes.

COX-2/sEH Dual Inhibitor PTUPB Potentiates the Anti-tumor Efficacy of Cisplatin

Fuli Wang^{1,2,a}, Hongyong Zhang^{1,a}, Ai-Hong Ma^{3,a}, Maike Zimmermann¹, Sung Hee Hwang⁴, Daniel Zhu¹, Tzu-yin Lin¹, Michael Malfatti⁵, Kenneth W Turteltaub⁵, Paul Henderson¹, Bruce D. Hammock⁴, Jianlin Yuan², Ralph W. de Vere White^{6,*} and Chong-Xian Pan^{1,6,7,*}

¹Department of Internal Medicine, School of Medicine, University of California, Sacramento CA 95817; ²Department of Urology, Xijing Hospital, The Fourth Military Medical University, Xi'an City, Shanxi Province, China, 710032; ³Department of Biochemistry and Molecular Medicine, School of Medicine, University of California, Sacramento CA 95817; ⁴Department of Entomology and Nematology, University of California, Davis, CA 95616; ⁵ Lawrence Livermore National Laboratory, Livermore, CA; ⁶Department of Urology, School of Medicine and Comprehensive Cancer Center, University of California, Sacramento CA 95817; ⁷VA Northern California Health Care System, Rancho Cordova, CA 95655.

^a Fuli Wang, Hongyong Zhang and Ai-Hong Ma contributed equally to this work.

* To whom correspondence should be addressed.

Chong-xian Pan, Email: cxpan@ucdavis.edu,

Ralph W. deVere White, Email: rwdeverewhite@ucdavis.edu,

4501 X Street, Room 3016

Sacramento, CA 95817

Tel: (916) 734-3771

Fax: (916) 734-7946.

LLNL-JRNL-741222

Running title: PTUPB Potentiates Cisplatin Anti-tumor Efficacy

Keywords: bladder cancer, PTUPB, cisplatin, patient-derived xenograft model

Funding: Work was supported in part by Merit Review (Award # I01 BX001784, C.-X. Pan) from the United States (U.S.) Department of Veterans Affairs Biomedical Laboratory Research and Development Program (The contents do not represent the views of the U.S. Department of Veterans Affairs or the United States Government); NCI Cancer Center Support Grant (PI: de Vere White; Grant #: 2 P30 CA 0933730); The Laney Foundation (PI: de Vere White); NIEHS grant R01 ES002710, NIEHS Superfund Research Program grant P42 ES04699, SBIR Phase II contract HHSN261201200048C (P.T. Henderson) and NIDDK grant R01 DK103616, National Institute of Neurological Disorders and Stroke (NINDS) U54 NS079202; The Research Resource for Biomedical AMS, National Institute of Health General Medical Sciences [2P41GM103483-16].

ABSTRACT

Cisplatin is highly toxic, but moderately effective in most cancers. Concurrent inhibition of cyclooxygenase-2 (COX-2) and soluble epoxide hydrolase (sEH) results in anti-tumor activity and has organ protective effects. The goal of this study was to determine the anti-tumor activity, toxicity and the underlying mechanisms of action of combination treatment with cisplatin and PTUPB, an orally available COX-2/sEH dual inhibitor. Immunodeficient NSG mice bearing bladder cancer patient-derived xenografts were treated with vehicle, PTUPB, cisplatin, or a combination. Median progression-free survival was 60.9 days in the PTUPB-cisplatin combination group, was highly significant compared to 31.3 days ($p<0.0001$) in the vehicle only control, 39.4 days ($p=0.007$) with single agent PTUPB and 47.0 days ($p=0.02$) with single agent cisplatin. Combination therapy was no more toxic than cisplatin only treatment as assessed by body weight, histochemical staining of major organs, blood counts and chemistry. Compared to controls, the combination increased apoptosis and decreased phosphorylation in the MAPK/ERK and PI3K/AKT/mTOR pathways. PTUPB treatment did not increase platinum-DNA adduct formation, which is the most critical step in platinum-induced cell death. The combination index method showed synergy between PTUPB and platinum agents in cell culture. In conclusion,

PTUPB potentiated the anti-tumor activity of cisplatin without increasing the toxicity *in vivo*, and has potential for further development as a combination chemotherapy partner.

INTRODUCTION

Cisplatin is the most commonly used chemotherapeutic agent in cancer treatment. However, it is only moderately effective in most cancer types and highly toxic (1). Cisplatin-based first-line combination therapy is associated with a response rate of approximately 50% for metastatic bladder cancer, and induces complete remission in less than 40% in the neoadjuvant setting for this disease (2). In advanced non-small cell lung cancer, the response rate of platinum-based combination therapy is less than 30% (3). Therefore, there is a great unmet need to develop novel therapies to potentiate efficacy and mitigate the toxicity of cisplatin (4).

One potential strategy to improve cisplatin therapy involves modulation of the arachidonic acid (ARA) pathway. This pathway plays numerous roles in inflammation and tumorigenesis. Eicosanoids are lipid mediators derived from ARA by cyclooxygenases (COXs), lipoxygenases (LOXs) and cytochrome P450s (CYPs). Among them, a COX-2 mediated metabolite, prostaglandin E₂ (PGE₂), is pro-inflammatory and pro-angiogenic (5). COX inhibitors, both nonsteroidal anti-inflammatory drugs (NSAIDs) and COX-2 selective inhibitors (coxibs), have been widely used to treat inflammation and pain. Separately, epoxyeicosatrienoic acids (EETs), derived from the metabolism of ARA by CYP epoxygenases, have potent anti-inflammatory, analgesic, antihypertensive, cardio-protective, and organ-protective properties (6-9). However, EETs are rapidly metabolized to inactive diols by soluble epoxide hydrolase (sEH) (10). sEH inhibitors (sEHI) maintain the level of EETs *in vivo*, and are now studied in clinical trials for various diseases. In preclinical studies as well as in clinical trials, a sEHI has displayed an excellent safety profile (11,12).

In addition, EETs transcriptionally inhibit the expression of COX-2 and thus decrease the production of PGE₂ (13). Interestingly, COX-2 overexpression in tumor or stromal cells leads to

tumor angiogenesis (14) and coxibs block the production of angiogenic factors, leading to inhibition of proliferation, migration, and vascular tube formation. However, targeting this single component of the ARA pathway with coxibs has failed in human clinical trials for several cancers (15-17). Furthermore, sEHIs synergize the analgesic and anti-inflammatory effects of coxibs (18,19), prevent the gastrointestinal erosion (20), and alter PGI₂ and TXB₂ ratios associated with blood clotting (18). Therefore, it is desirable to inhibit both COX-2 and sEH in order to maximize antitumor activity and reduce toxic effects of selective COX-2 inhibition. This dual COX-2/sEH inhibition strategy also may have the potential to protect normal tissues from cisplatin toxicity.

We recently demonstrated that combination treatment of celecoxib and an sEH inhibitor *t*-AUCB has synergistic effects on blocking angiogenesis and tumorigenesis in two mouse models of cancer (21-24). Based on these findings, we developed single compound that concurrently inhibits both COX-2 and sEH called (4-(5-phenyl-3-{3-[3-(4-trifluoromethyl-phenyl)-ureido]-propyl}-pyrazol-1-yl)-benzenesulfonamide; PTUPB) (**Figure S1**) (25). This compound is more effective at inhibiting primary tumor growth and metastasis compared to inhibitors selective to either pathway, either as single agents or in combination. PTUPB acts, in part, by suppressing tumor angiogenesis via selective inhibition of endothelial cell proliferation, without any obvious cytotoxic effects (26).

Here we report interaction of cisplatin with PTUPB. We hypothesized that combination of PTUPB and cisplatin achieved synergistic anti-tumor activity without increasing cisplatin toxicity. Here we extended our work to include immunodeficient nod scid gamma (NSG) mice carrying patient-derived xenograft (PDX) model of bladder cancer, and conducted additional mechanistic studies (27). We observed that *in vivo* PTUPB potentiated cisplatin efficacy without

increasing toxicity. Platinum-DNA adducts were not modulated by PTUPB exposure, indicating a completely independent mechanism of action. However, PTUPB enhances apoptosis and downregulates proliferation signaling.

MATERIALS AND METHODS

Materials and Supplies

A bladder cancer patient-derived xenograft (PDX) model was provided by The Jackson Laboratory (JAX, Bar Harbor, ME). PDX was developed through subcutaneous implantation from clinical tumor tissues into immunodeficient NOD.Cg-*Prkdc*^{scid} *Il2rg*^{tm1Wjl}/SzJ (NSG; JAX strain #5557) female mice, followed by serial *in vivo* passaging as we previously described (27). All experiments utilized PDX models within the first five passages. Cisplatin was purchased from (EMD Biosciences, Inc., San Diego, CA). [¹⁴C]carboplatin was purchased from GE Healthcare (Waukesha, WI) and was prepared as described (28). PTUPB was synthesized as previously described (25). The bladder cancer cell line 5637 was purchased from American Type Culture Collection (ATCC, Manassas, VA) and was cultured with the RPMI-1640 medium supplemented with 10% fetal bovine serum (Gibco, Grand Island, NY) and 1% penicillin-streptomycin (Gibco, Grand Island, NY) and incubated at 37°C under 5% CO₂.

PDX bladder cancer

All NSG PDX studies were performed at the University of California Davis with IACUC approval (Protocol # 17794). Experiments were carried out in 6 to 9 week old female NSG mice bearing bladder cancer PDX (ID# BL0293; JAX Model # TM00016). When the tumors achieved volumes of 150~200 mm³, mice were randomized to four groups (n = 8 mice per group) as

follows: a vehicle group (PEG 400, 10ml/kg, oral), a PTUPB group, a cisplatin group, and a combination of PTUPB and cisplatin group. PTUPB (30 mg/kg in PEG 400) was daily administered once per day by oral gavage. Cisplatin (1 mg) was diluted in 1 mL of 0.9 % saline and administered at a dose of 2 mg/kg (IV, tail vein, once per day) on days 1, 2, 3, 14, 15 and 16. Animal weight and tumor size were measured twice per week. The tumor volume was calculated with the following formula: length (mm) \times width (mm) \times width (mm) \times 0.5. The percentage of tumor growth inhibition (TGI) was calculated as follows;

$$100\% \times (1 - [(V_{\text{treated}(\text{final day})} - V_{\text{treated}(\text{initial day})}) / (V_{\text{control}(\text{final day})} - V_{\text{control}(\text{initial day})})]),$$

where V is tumor volume.

On days 6 and 20, two mice from each group were sacrificed; complete blood count (CBC), blood urea nitrogen (BUN), aspartate aminotransferase (AST), creatinine and potassium in blood samples collected from those mice were analyzed at the Veterinary Medicine Comparative Pathology Laboratory of University of California Davis. The tumor, heart, liver, spleen, lung and kidney were harvested 1 hr after the final treatment and the tissue samples were fixed in formalin or were frozen at -80°C. Tumor sections were stained with hematoxylin and eosin (H&E) or were used for immunohistochemistry analysis. A board-certified pathologist provided detailed interpretation of tumor histomorphology and scoring of immunohistochemical staining. Some of the tumor sections were lysed and chromatographed using SDS-PAGE followed by transfer onto a PVDF membrane. The membranes were blocked in 5% nonfat dry milk for 1 h at room temperature, and probed with p-AKT(S473) and p-ERK(Thr202/Tyr204) antibodies (Cell Signaling Technology, Beverly, MA) and rabbit monoclonal anti-GAPDH antibody (Cell

Signaling Technology, Beverly, MA). The membranes were then probed with horseradish peroxidase (HRP) tagged secondary antibodies. The secondary antibodies on the blot were detected by an ECL Plus Western Blotting Detection Reagent (GE Healthcare, Piscataway, NJ). Apoptosis was detected with anti-cleaved caspase-3 antibody (Cell Signaling, Danvers, MA) according to the manufacturer's protocol.

Accelerator mass spectrometry to determine platinum-DNA adduct formation

The ATCC 5637 bladder cancer cell line and NSG-PDX mice were used to assess the impact of PTUPB on ¹⁴C-labeled carboplatin-DNA adduct formation.

Carboplatin-DNA adduct formation in vitro. For cell culture studies, 60-mm dishes of 5637 cell cultures were either pretreated with 10 μ M PTUPB for 5 hr followed by 100 μ M [¹⁴C]carboplatin (36,000 dpm/mL), or simultaneously dosed with PTUPB and [¹⁴C]carboplatin. Four hours after carboplatin was added, the cells were washed with PBS. The 4 hr incubation time was chosen due to the *in vivo* carboplatin half-life (1.3-6 hr) in patients. Cells were harvested at the 4 hr time point in one group of dishes and another group was washed and further incubated for 20hr with fresh drug-free medium before cell harvest in order to determine DNA repair. Cell pellets were stored at -80°C until DNA extraction.

Carboplatin-DNA adduct formation in vivo. NSG PDX mice were dosed with 10 μ L/g of 37.5 mg/kg [¹⁴C]carboplatin (50,000 dpm/g) via IV bolus injection. PTUPB (30 mg/kg in PEG 400) was administered via oral gavage 1hr or 16 hr before carboplatin dosing. Mice were sacrificed and tumor tissues harvested 24 hours after carboplatin dosing. DNA was extracted using a Promega Wizard genomic DNA purification kit according to manufacturer's instructions.

Ten micrograms of DNA per sample was submitted to Lawrence Livermore National Laboratory (LLNL) for AMS analysis as previously reported (29).

Median effect analysis to determine *in vitro* drug-drug interaction

The method published by Chou and Talalay was used to determine the extent and nature (synergism, additivity and antagonism) of PTUPB and cisplatin interaction (30,31). The drugs were combined in various concentration ratios, given to cultured 5637 cells followed by cell survival determination. The resulting data were used to calculate a combination index (*CI*).

Statistics

Data are presented as mean \pm standard error of the mean (SEM). Group comparisons were carried out using one-way analysis of variance or Student's *t* test. Survival analysis was performed using the Kaplan-Meier method. A *p* value of less than 0.05 was considered statistically significant.

RESULTS

Co-administration of PTUPB potentiated the anti-tumor activity of cisplatin

We previously showed PTUPB had anti-tumor activity in mouse Lewis lung cancer (LLC) and NDL (Her2⁺, Ki67⁺, ER/PR negative) breast carcinoma models. Here, we determined whether PTUPB possessed any anti-tumor activity in human bladder cancer cells and tumors, and synergized with cisplatin treatment. We used the bladder cancer patient-derived xenograft (PDX) model BL0293, a tumor type that, like most bladder cancers in clinic, is only moderately sensitive to cisplatin (27). Treatment with single agent PTUPB or cisplatin exhibited moderate

anti-tumor activity in mice bearing BL0293 tumors (**Figure 1**). The time required to reach a 7.5 fold increase in tumor volume was used as a reasonably attainable endpoint for this study. Since treatment was started when the PDX tumor volume reached 100-200 mm³, a 7.5 fold increase represented a final tumor volume of no more than 1.5 cm³, a humane endpoint. Vehicle only control had a median time to a 7.5-fold increase in tumor volume of 20.0 days, whereas the endpoint was achieved in 24.4 days (p = 0.085) and 35.8 days (p = 0.0003) for the PTUPB and cisplatin monotherapy groups, respectively. The median time to endpoint in the cisplatin-PTUPB combination group was significantly longer (60.9 days) than that of either PTUPB (p = 0.007) or cisplatin (p = 0.02) group (**Figures 1A**). Analysis of the median survival showed that single agent PTUPB did not significantly increase survival time compared to control (39.4 days vs. 31.3 days, p = 0.201), whereas single agent cisplatin treatment extended survival to 47.0 days (p = 0.004). The survival time could be further significantly increased by co-treatment of mice with PTUPB and cisplatin to 60.9 days, which was longer than that of either the PTUPB (p = 0.007) or cisplatin (p = 0.02) monotherapy groups (**Figures 1B**).

Even though PTUPB potentiated the anti-tumor efficacy of cisplatin, we did not observe any significant increase in toxicity. Comparing to vehicle control, PTUPB monotherapy slightly decreased body weight (p = 0.086 at day 23; p = 0.118 at day 30) while cisplatin treatment led to significant weight loss (p=0.00009 at day 23; p = 0.008 at day 30). The addition of PTUPB to cisplatin therapy did not further increase the weight loss (**Figure S2**). We also determined complete blood cell count (CBC) and chemistry panels at day 6 and 20 of treatment (**Figure S3-4**). No significant difference in blood panel data was observed among all treatment groups compared to the controls. Histology examination of major organs at day 20 revealed cisplatin and combination treatment induced swollen distal tubule cells in kidneys, and cytoplasmic

vacuolization (microvesicular steatosis) in the hepatocytes. Although these changes were consistent with cisplatin toxicity, they were modest and could be due to normal variations in tissue morphology. However, no such morphology changes were observed in the control and PTUPB monotherapy groups, suggesting that they might be caused by cisplatin. No other histological changes were observed in other organs (**Figure S5**).

Combination treatment of cisplatin and PTUPB inhibited proliferation and induces apoptosis in bladder cancer xenografts

Ki-67 is a nuclear non-histone protein that is expressed among dividing but not in resting cells, and is frequently used to assess the proliferation state of tissues. The determination of cleaved caspase 3 is commonly used as an indicator of apoptosis. The combination of cisplatin with PTUPB treatment led to a significant decrease of Ki-67 expression and substantial increase of cleaved caspase-3 in stained tumor tissues when compared to single treatment with PTUPB or cisplatin (**Figure 2 and Figure S6**). These data demonstrate that the anti-tumor activity of the combination treatment with PTUPB and cisplatin was, at least in part, due to decreased cell proliferation and increased apoptosis.

Combination treatment of cisplatin and PTUPB significantly reduced signaling pathways essential for cell growth

The MAPK/ERK and PI3K/AKT/mTOR signaling pathways are shared by many receptor tyrosine kinases and often essential for tumor growth and survival. To determine how the different treatments affected these two signaling pathways, tumor tissues were collected at day 3 after treatment started, and at day 17 when tumors started to regrow in the PTUPB and cisplatin

groups or were stabilized as in the combination group. While treatment with either PTUPB alone or cisplatin alone did not significantly diminish levels of either phosphorylated activated ERK (p-ERK) or AKT (p-AKT), the combination treatment of PTUPB and cisplatin substantially decreased levels of both p-ERK and p-AKT at day 3. On Day 17, increased levels of p-ERK and p-AKT were observed in the PTUPB and cisplatin combination group (**Figure 3**). The p-Erk and p-Akt levels were increased by 2.45 (1.20/0.49) and 78.5 (1.57/0.02) times, respectively. These data confirmed that combined therapy suppressed bladder cancer growth, at least in part, through these two pathways, while pathway reactivation was associated with tumor adaptation and re-growth.

PTUPB did not alter platinum-DNA adduct formation

As alkylating agents, platinum-based drugs (including cisplatin and carboplatin) kill cancer cells through formation of covalent drug-DNA adducts. Hence we determined whether PTUPB potentiated the anti-tumor activity of cisplatin agents via increasing DNA adducts by using [¹⁴C]carboplatin-DNA adducts as a surrogate marker that is amenable to AMS analysis. AMS is ultrasensitive for quantification of ¹⁴C in biological sample, and was used to measure carboplatin-DNA adduct formation under physiologically relevant drug concentrations (32). Since cisplatin does not have any carbon atoms in the molecule, it cannot be labeled with ¹⁴C. Since both cisplatin and carboplatin form the same therapeutically relevant drug-DNA diadducts and share a similar resistance spectrum (33), we used [¹⁴C]carboplatin for this part of the study.

First, we determined the effect of PTUPB on carboplatin-DNA adduct formation in cell culture with the ATCC 5637 bladder cancer cell line (34). Cultures of 5637 cells were treated with either carboplatin (100 μ M) alone or a combination of carboplatin (100 μ M) and PTUPB

(10 μ M). The 100 μ M concentration of carboplatin was used based on its maximum blood concentration in patients after chemotherapy and the treatment duration of 4 hours was chosen to simulate carboplatin plasma half-life of 1.5-6.0 hours in patients. PTUPB exposure did not significantly alter platinum-DNA adduct formation after 4h (528 ± 41 adducts per 10^8 nt with the carboplatin alone versus 593 ± 282 adducts per 10^8 nt with the combination treatment, $p = 0.713$) (**Figure 4A**). Similarly, pretreatment of cells with 10 μ M PTUPB for 5 hours followed by the addition of carboplatin did not alter the carboplatin induced DNA adduct formation (706 ± 26 adducts per 10^8 nt with the carboplatin alone versus 606 ± 66 adducts per 10^8 nt with the PTUPB pretreatment ($p = 0.071$) (**Figure 4B**). Clearly, PTUPB did not impact drug-target binding and metabolism of carboplatin in cell culture.

We next determined whether PTUPB affected the repair of carboplatin-DNA adducts since increased DNA repair is one of the major mechanisms of cellular resistance to platinum-based cancer therapy. To perform this experiment, 5637 cell cultures were treated with carboplatin alone or with PTUPB plus carboplatin combination for 4 hours followed by removal of both drugs, washing and additional culture with drug-free medium for 20 hours. At 24 hours, the platinum-DNA adduct levels were not significantly different in the two treatment groups, suggesting no difference of DNA repair between two treatments.

We also determined whether PTUPB influenced carboplatin-DNA adduct levels *in vivo* (**Figure 4C**). PTUPB was administered either 16 hours or 1 hour before carboplatin injection and tumors were collected 24 hours after carboplatin treatment. Carboplatin-DNA adduct levels from isolated tumor DNA showed no significant difference between tumors that were treated with carboplatin alone, 16 hours of PTUPB ($p = 0.856$) or 1 hour PTUPB ($p = 0.362$) pre-treatment (1070 ± 317 adducts per 10^8 nt, 1019 ± 434 adducts per 10^8 nt, and 1334 ± 384 adducts

per 10^8 nt, respectively). The *in vivo* data are fully consistent with the cell line data, and support PTUPB having a fully orthogonal mechanism of action compared to carboplatin and likely cisplatin.

PTUPB and the platinum drug cisplatin showed synergistic drug-drug interaction

Since we showed PTUPB potentiated the anti-tumor effect of cisplatin *in vivo* in a bladder PDX model, we wanted to further study the mechanism of the combination effect of these two drugs *in vitro*. To address this question, the combination index (*CI*) method (31) was used to determine the drug-drug interaction of PTUPB and cisplatin. First, we determined the effect of single drug treatment on 5637 bladder cancer cells (**Figure 5A**). Cultures of 5637 cells were treated with increasing concentrations of PTUPB or cisplatin (0, 0.01, 0.1, 1, 2, 5, 10, 20, 50, 100 μ M). The IC_{50} of cisplatin and PTUPB on 5637 cells are 4.1 μ M and 90.4 μ M, respectively. Next, we determined the combination drug effect of PTUPB and cisplatin (**Figure 5B**). 5637 cells were treated with different concentrations of cisplatin (0, 0.01, 0.1, 0.5, 1, 2, 5, 10, 100 μ M) in combination with different concentrations of PTUPB (1, 2, 5, 10 μ M). The *CI* values of cisplatin and PTUPB are shown in **Table 1**. PTUPB at concentrations of 1, 2, 5 and 10 μ M showed significant synergistic effects in combination with cisplatin.

DISCUSSION

Based on our findings of improved analgesic, anti-inflammatory and anti-cancer efficacy of the co-inhibition of sEH and COX-2, we developed the COX-2/sEH dual inhibitor PTUPB (**SI-1**) (9).

We demonstrated kidney protection and blood pressure attenuation by PTUPB in 8-week study in type 2 diabetic Zucker Diabetic Fatty (ZDF) rats (35). In addition, we previously demonstrated that PTUPB suppressed primary breast tumor growth and metastasis (26). The previous work was focused on PTUPB as a single agent. Here we showed that PTUPB potentiated the *in vivo* anti-tumor activity of cisplatin, possibly via a synergistic interaction. All of these attributes make PTUPB an attractive candidate for further development as a combination chemotherapy partner.

PTUPB potentiated the anti-tumor activity of cisplatin without increasing the toxicity in mice carrying bladder cancer PDXs. The use of PDX mouse models enables the study of potential drug candidates in a model system that more closely resembles the clinical patient setting as compare to establishing xenografts from cultured cancer cells or cell lines. PDX are developed from unselected and uncultured human clinical cancer tissues. They maintain tumor morphology and 92-97% genetic fidelity of their parental cancers (27). In contrast to frequent discordant of drug sensitivity between cell lines and clinical cancer response (36-38), there is high concordance of cancer response between PDXs and patients (39). Therefore, the findings in this study can likely to be translated into clinical applications.

NSAIDs are often used to reduce pain in cancer patients. It has been observed that the combination of sEH inhibitors with coxibs displays significant synergistic anti-inflammatory and analgesic effects in inflammatory animal models (18). Furthermore, stabilization of EET levels by sEHI indirectly inhibits COX-2 (40) and suppresses COX-2 transcription (18). Previously our work showed that co-administration of celecoxib and a sEH inhibitor synergistically inhibited tumor growth in primary Lewis lung carcinoma (LLC) and spontaneous lung metastasis in mice (26). Moreover, systemic co-administration of a sEH inhibitor with a lower dose of coxibs

resulted in significant reduction in the adverse side effects of NSAIDs and coxibs on gastrointestinal erosion, the cardiovascular system and kidneys, while maintaining efficacy in reducing pain and inflammation (20).

Here we not only show that PTUPB enhanced cisplatin efficacy, but also explored the underlying mechanisms of potentiation. The increased efficacy was not due to increased drug-DNA adduct formation. We gathered evidence that the potentiation is possibly due to *in vivo* factors, such as angiogenesis, and reduced activation of proliferation including the AKT and ERK signaling pathways. Treatment of cisplatin and PTUPB decreased the levels of both p-ERK and p-AKT in tumor xenografts, suggesting that these two major signaling pathways were down regulated. We previously reported the evidence of anti angiogenic properties of PTUPB (26).

PTUPB could be a breakthrough for improving platinum-based chemotherapy. Even though targeted therapy and immunotherapy have emerged as promising therapeutic modalities, cytotoxic chemotherapy will still be the mainstay in the foreseeable future. For example, targeted and immunotherapies benefit only a minority of patients with non-small cell lung and bladder cancers. The response rate of immunotherapy in both cancers is less than 20% (41,42). In conclusion, the COX2/sEH dual inhibitor PTUPB potentiates and possibly synergizes cisplatin in bladder cancer PDXs *in vivo* without increasing toxicity.

In conclusion, the COX2/sEH dual inhibitor PTUPB synergizes cisplatin in targeting bladder cancer PDXs *in vivo* without increasing toxicity. PTUPB and cisplatin treatment increases apoptosis and decreases the activity of the AKT and ERK pathways, but does not increase the formation of platinum-DNA adducts, the most critical step of platinum-induced cell death.

ACKNOWLEDGMENTS

We also would like to thank Tsung-Chieh Shih for technical assistance in IHC staining, Jun Yang, Christopher Morisseau, Dipak Panighy, and Ted Ognibene for technical support in conducting the experiments, and George Cimino for help during manuscript preparation. Portions of the work was performed under the auspices of the U.S. DOE by LLNL under Contract DE-AC52-07NA27344.

REFERENCES

1. Ho GY, Woodward N, Coward JI. Cisplatin versus carboplatin: comparative review of therapeutic management in solid malignancies. *Critical reviews in oncology/hematology* **2016**;102:37-46 doi 10.1016/j.critrevonc.2016.03.014.
2. Kamat AM, Hahn NM, Efstathiou JA, Lerner SP, Malmstrom PU, Choi W, *et al.* Bladder cancer. *Lancet* **2016** doi 10.1016/S0140-6736(16)30512-8.
3. Rizvi NA, Hellmann MD, Brahmer JR, Juergens RA, Borghaei H, Gettinger S, *et al.* Nivolumab in Combination With Platinum-Based Doublet Chemotherapy for First-Line Treatment of Advanced Non-Small-Cell Lung Cancer. *Journal of clinical oncology : official journal of the American Society of Clinical Oncology* **2016**;34(25):2969-79 doi 10.1200/JCO.2016.66.9861.
4. Grivas PD, Day KC, Karatsinides A, Paul A, Shakir N, Owainati I, *et al.* Evaluation of the antitumor activity of dacomitinib in models of human bladder cancer. *Molecular medicine* **2013**;19:367-76 doi 10.2119/molmed.2013.00108.
5. Xu L, Stevens J, Hilton MB, Seaman S, Conrads TP, Veenstra TD, *et al.* COX-2 inhibition potentiates antiangiogenic cancer therapy and prevents metastasis in preclinical models. *Science translational medicine* **2014**;6(242):242ra84 doi 10.1126/scitranslmed.3008455.
6. Morisseau C, Hammock BD. Impact of soluble epoxide hydrolase and epoxyeicosanoids on human health. *Annual review of pharmacology and toxicology* **2013**;53:37-58 doi 10.1146/annurev-pharmtox-011112-140244.
7. Spector AA, Norris AW. Action of epoxyeicosatrienoic acids on cellular function. *American journal of physiology Cell physiology* **2007**;292(3):C996-1012 doi 10.1152/ajpcell.00402.2006.
8. Inceoglu B, Jinks SL, Ulu A, Hegedus CM, Georgi K, Schmelzer KR, *et al.* Soluble epoxide hydrolase and epoxyeicosatrienoic acids modulate two distinct analgesic pathways. *Proceedings of the National Academy of Sciences of the United States of America* **2008**;105(48):18901-6 doi 10.1073/pnas.0809765105.
9. Shen HC, Hammock BD. Discovery of inhibitors of soluble epoxide hydrolase: a target with multiple potential therapeutic indications. *Journal of medicinal chemistry* **2012**;55(5):1789-808 doi 10.1021/jm201468j.

10. Spector AA, Fang X, Snyder GD, Weintraub NL. Epoxyeicosatrienoic acids (EETs): metabolism and biochemical function. *Progress in lipid research* **2004**;43(1):55-90.
11. Chen D, Whitcomb R, MacIntyre E, Tran V, Do ZN, Sabry J, et al. Pharmacokinetics and pharmacodynamics of AR9281, an inhibitor of soluble epoxide hydrolase, in single- and multiple-dose studies in healthy human subjects. *Journal of clinical pharmacology* **2012**;52(3):319-28 doi 10.1177/0091270010397049.
12. Lazaar AL, Yang L, Boardley RL, Goyal NS, Robertson J, Baldwin SJ, et al. Pharmacokinetics, pharmacodynamics and adverse event profile of GSK2256294, a novel soluble epoxide hydrolase inhibitor. *British journal of clinical pharmacology* **2016**;81(5):971-9 doi 10.1111/bcp.12855.
13. Schmelzer KR, Kubala L, Newman JW, Kim IH, Eiserich JP, Hammock BD. Soluble epoxide hydrolase is a therapeutic target for acute inflammation. *Proceedings of the National Academy of Sciences of the United States of America* **2005**;102(28):9772-7 doi 10.1073/pnas.0503279102.
14. Ghosh N, Chaki R, Mandal V, Mandal SC. COX-2 as a target for cancer chemotherapy. *Pharmacological reports : PR* **2010**;62(2):233-44.
15. Gridelli C, Gallo C, Ceribelli A, Gebbia V, Gamucci T, Ciardiello F, et al. Factorial phase III randomised trial of rofecoxib and prolonged constant infusion of gemcitabine in advanced non-small-cell lung cancer: the GEmitabine-COxib in NSCLC (GECO) study. *The Lancet Oncology* **2007**;8(6):500-12 doi 10.1016/S1470-2045(07)70146-8.
16. Groen HJ, Sietsma H, Vincent A, Hochstenbag MM, van Putten JW, van den Berg A, et al. Randomized, placebo-controlled phase III study of docetaxel plus carboplatin with celecoxib and cyclooxygenase-2 expression as a biomarker for patients with advanced non-small-cell lung cancer: the NVALT-4 study. *Journal of clinical oncology : official journal of the American Society of Clinical Oncology* **2011**;29(32):4320-6 doi 10.1200/JCO.2011.35.5214.
17. Pan CX, Loehrer P, Seitz D, Helft P, Julian B, Ansari R, et al. A phase II trial of irinotecan, 5-fluorouracil and leucovorin combined with celecoxib and glutamine as first-line therapy for advanced colorectal cancer. *Oncology* **2005**;69(1):63-70 doi 10.1159/000087302.
18. Schmelzer KR, Inceoglu B, Kubala L, Kim IH, Jinks SL, Eiserich JP, et al. Enhancement of antinociception by coadministration of nonsteroidal anti-inflammatory drugs and soluble epoxide hydrolase inhibitors. *Proceedings of the National Academy of Sciences of the United States of America* **2006**;103(37):13646-51 doi 10.1073/pnas.0605908103.
19. Wagner K, Inceoglu B, Hammock BD. Soluble epoxide hydrolase inhibition, epoxyenated fatty acids and nociception. *Prostaglandins & other lipid mediators* **2011**;96(1-4):76-83 doi 10.1016/j.prostaglandins.2011.08.001.
20. Goswami SK, Wan D, Yang J, Trindade da Silva CA, Morisseau C, Kodani SD, et al. Anti-Ulcer Efficacy of Soluble Epoxide Hydrolase Inhibitor TPPU on Diclofenac-Induced Intestinal Ulcers. *The Journal of pharmacology and experimental therapeutics* **2016**;357(3):529-36 doi 10.1124/jpet.116.232108.
21. Panigrahy D, Edin ML, Lee CR, Huang S, Bielenberg DR, Butterfield CE, et al. Epoxyeicosanoids stimulate multiorgan metastasis and tumor dormancy escape in mice. *The Journal of clinical investigation* **2012**;122(1):178-91 doi 10.1172/JCI58128.
22. Zhang G, Panigrahy D, Mahakian LM, Yang J, Liu JY, Stephen Lee KS, et al. Epoxy metabolites of docosahexaenoic acid (DHA) inhibit angiogenesis, tumor growth, and metastasis. *Proceedings of the National Academy of Sciences of the United States of America* **2013**;110(16):6530-5 doi 10.1073/pnas.1304321110.
23. Wang D, Dubois RN. Eicosanoids and cancer. *Nature reviews Cancer* **2010**;10(3):181-93 doi 10.1038/nrc2809.
24. Panigrahy D, Kalish BT, Huang S, Bielenberg DR, Le HD, Yang J, et al. Epoxyeicosanoids promote organ and tissue regeneration. *Proceedings of the National*

Academy of Sciences of the United States of America **2013**;110(33):13528-33 doi 10.1073/pnas.1311565110.

25. Hwang SH, Wagner KM, Morisseau C, Liu JY, Dong H, Wecksler AT, *et al.* Synthesis and structure-activity relationship studies of urea-containing pyrazoles as dual inhibitors of cyclooxygenase-2 and soluble epoxide hydrolase. *Journal of medicinal chemistry* **2011**;54(8):3037-50 doi 10.1021/jm2001376.
26. Zhang G, Panigrahy D, Hwang SH, Yang J, Mahakian LM, Wettersten HI, *et al.* Dual inhibition of cyclooxygenase-2 and soluble epoxide hydrolase synergistically suppresses primary tumor growth and metastasis. *Proceedings of the National Academy of Sciences of the United States of America* **2014**;111(30):11127-32 doi 10.1073/pnas.1410432111.
27. Pan CX, Zhang H, Tepper CG, Lin TY, Davis RR, Keck J, *et al.* Development and Characterization of Bladder Cancer Patient-Derived Xenografts for Molecularly Guided Targeted Therapy. *PLoS one* **2015**;10(8):e0134346 doi 10.1371/journal.pone.0134346.
28. Zimmermann M, Wang S, Zhang H, Lin T, Malfatti M, Haack K, *et al.* Microdose-induced Drug-DNA Adducts as Biomarkers of Chemotherapy Resistance in Humans and Mice. *Molecular Cancer Therapeutics* **2016**.
29. Ognibene TJ, Bench G, Vogel JS, Peaslee GF, Murov S. A high-throughput method for the conversion of CO₂ obtained from biochemical samples to graphite in septa-sealed vials for quantification of ¹⁴C via accelerator mass spectrometry. *Analytical chemistry* **2003**;75(9):2192-6 doi 10.1021/ac026334j.
30. Chou TC. Theoretical basis, experimental design, and computerized simulation of synergism and antagonism in drug combination studies. *Pharmacological reviews* **2006**;58(3):621-81 doi 10.1124/pr.58.3.10.
31. Chou TC. Drug combination studies and their synergy quantification using the Chou-Talalay method. *Cancer research* **2010**;70(2):440-6 doi 10.1158/0008-5472.CAN-09-1947.
32. Henderson PT, Li T, He M, Zhang H, Malfatti M, Gandara D, *et al.* A microdosing approach for characterizing formation and repair of carboplatin-DNA monoadducts and chemoresistance. *International journal of cancer* **2011**;129(6):1425-34 doi 10.1002/ijc.25814.
33. Henderson PT, Pan CX. Human microdosing for the prediction of patient response. *Bioanalysis* **2010**;2(3):373-6 doi 10.4155/bio.10.3.
34. Wang S, Zhang H, Scharadin TM, Zimmermann M, Hu B, Pan AW, *et al.* Molecular Dissection of Induced Platinum Resistance through Functional and Gene Expression Analysis in a Cell Culture Model of Bladder Cancer. *PLoS one* **2016**;11(1):e0146256 doi 10.1371/journal.pone.0146256.
35. Hye Khan MA, Hwang SH, Sharma A, Corbett JA, Hammock BD, Imig JD. A dual COX-2/sEH inhibitor improves the metabolic profile and reduces kidney injury in Zucker diabetic fatty rat. *Prostaglandins & other lipid mediators* **2016**;125:40-7 doi 10.1016/j.prostaglandins.2016.07.003.
36. McDermott U, Sharma SV, Dowell L, Greninger P, Montagut C, Lamb J, *et al.* Identification of genotype-correlated sensitivity to selective kinase inhibitors by using high-throughput tumor cell line profiling. *Proceedings of the National Academy of Sciences of the United States of America* **2007**;104(50):19936-41 doi 10.1073/pnas.0707498104.
37. Barretina J, Caponigro G, Stransky N, Venkatesan K, Margolin AA, Kim S, *et al.* The Cancer Cell Line Encyclopedia enables predictive modelling of anticancer drug sensitivity. *Nature* **2012**;483(7391):603-7 doi 10.1038/nature11003.
38. Johnson JI, Decker S, Zaharevitz D, Rubinstein LV, Venditti JM, Schepartz S, *et al.* Relationships between drug activity in NCI preclinical in vitro and in vivo models and

early clinical trials. *British journal of cancer* **2001**;84(10):1424-31 doi 10.1054/bjoc.2001.1796.

- 39. Garralda E, Paz K, Lopez-Casas PP, Jones S, Katz A, Kann LM, *et al.* Integrated next-generation sequencing and avatar mouse models for personalized cancer treatment. *Clinical cancer research : an official journal of the American Association for Cancer Research* **2014**;20(9):2476-84 doi 10.1158/1078-0432.CCR-13-3047.
- 40. Kozak W, Aronoff DM, Boutaud O, Kozak A. 11,12-epoxyeicosatrienoic acid attenuates synthesis of prostaglandin E2 in rat monocytes stimulated with lipopolysaccharide. *Experimental biology and medicine (Maywood, NJ)* **2003**;228(7):786-94.
- 41. Powles T, Eder JP, Fine GD, Braiteh FS, Loriot Y, Cruz C, *et al.* MPDL3280A (anti-PD-L1) treatment leads to clinical activity in metastatic bladder cancer. *Nature* **2014**;515(7528):558-62 doi 10.1038/nature13904.
- 42. Borghaei H, Paz-Ares L, Horn L, Spigel DR, Steins M, Ready NE, *et al.* Nivolumab versus Docetaxel in Advanced Nonsquamous Non-Small-Cell Lung Cancer. *The New England journal of medicine* **2015**;373(17):1627-39 doi 10.1056/NEJMoa1507643.

Figure Legends

Figure 1: Potentiation of cisplatin anti-tumor activity by PTUPB. A). Tumor growth in the NSG-PDX bladder cancer mouse model. When the volume of the tumor xenografts reached approximately 0.1~0.2 cm³, mice were treated with PEG 400 control, single agent cisplatin (2 mg/kg, i.v., Day 1, 2, 3, 14, 15, and 16, red arrows), single agent PUTUPB (30 mg/kg, orally, once daily), and cisplatin (2 mg/kg) plus PUTUB (30 mg/kg) combination. The tumor dimensions were measured every 3~4 days. The tumor volume was calculated using the formula: $0.5 \times \text{length} \times \text{width}^2$ (mm³). Mice were euthanized when the tumor volume reached 1.5~2 cm³ (~7.5 times the baseline volume or 7.5 \times BL). The median time of the tumor growth to 7.5 \times BL (blue dotted line) was 20 days for the control and 24.4 days in the PTUPB group ($p=0.085$) and 35.8 days in the cisplatin group ($p=0.0003$). The median time to endpoint in the cisplatin and PTUPB combination group was significantly increased to 47.8 days compared to PTUPB ($p<0.0001$) or cisplatin ($p=0.002$) monotherapy groups. **B).** Median survival with statistical analysis. Median survival of the combination treatment group was 60.9 days, significantly longer than that of either PTUPB (39.4 days, $p=0.007$) or cisplatin (47 days, $p=0.02$) monotherapy groups.

Figure 2: Ki-67 and caspase-3 expression as determined by immunohistochemical (IHC) analysis. Formalin-fixed paraffin-embedded xenograft sections were stained for H&E, Ki-67 and caspase-3. Left panel: Hematoxylin and eosin stain (H & E stain). Middle panel: Ki-67 staining. More Ki-67 positive cells were observed in the control group, but significantly decreased in the combination group. Right Panel: cleaved Caspase-3. Compared with the

control group, increasing numbers of cells stained positive for active caspase-3 in the PTUPB plus Cisplatin combination group.

Figure 3: Effect of PTUPB and cisplatin on cell signaling pathways. A). Western blot analysis of protein expression of indicated phospho-proteins and loading control GAPDH. Protein was extracted at indicated times from PDX BL0293 tumors treated with cisplatin, PTUPB or cisplatin-PTUPB combination therapy. The numbers indicate the ratio of band density relative to its control after normalization with GAPDH.

B). Illustration of signaling pathways.

Figure 4: PTUPB did not alter carboplatin-DNA adduct formation. A). Cultures of the ATCC bladder cancer cell line 5637 were incubated with 100 μ M [14 C]carboplatin in the presence (gray bar) or absence (white bar) of 10 μ M PTUPB for 4h or 4h then washed and further incubated 20hr with fresh drug-free culture medium. **B).** 5637 cells were pretreated (grey bar) with 10 μ M PTUPB for 5h before cells were exposed to 100 μ M [14 C]carboplatin for indicated amount of time. **C).** NSG mice carrying BL0293 tumors were treated with 37.5 mg/kg (therapeutic dose) carboplatin (50,000 dpm/g) via IV bolus and tissue was harvested after 24hr. PTUPB (30 mg/kg in PEG400) was administered via oral gavage 16hr (grey bar) or 1hr (black bar) before carboplatin dosing.

Figure 5: Effect of PTUPB and cisplatin on bladder cancer cells. Dose-response curves of 5637 cells treated with cisplatin and PTUPB at different concentrations as determined in a 72hr cell viability assay. A). Single drug treatment. Cultures of 5637 cells were treated with different concentrations of PTUPB or cisplatin (0, 0.01, 0.1, 1, 2, 5, 10, 20, 50, 100 μ M). **B).**

Combination drugs treatment. 5637 cells were treated with different concentrations of cisplatin (0, 0.01 0.1, 0.5, 1, 2, 5, 10, 100 uM) in combination with different concentrations of PTUPB (1, 2, 5, 10 μ M).

Table 1. Drug-drug interaction between PTUPB and Cisplatin. Combination index values at different concentrations of PTUPB and cisplatin in 5637 bladder cancer cells.

Figure S1. The chemical structure of a COX-2/sEH dual inhibitor, 4-(5-phenyl-3-[3-(4-trifluoromethyl-phenyl)-ureido]-propyl}-pyrazol-1-yl)-benzenesulfonamide (PTUPB).

Figure S2. Body weight change during PDX bladder cancer mice experiment. Compared to the control group, PTUPB slightly decreased body weight while cisplatin treatment led to more weight loss. Addition of PTUPB did not further increase the weight loss. No significant behavioral abnormality was observed among any of these groups. N=8 mice per group.

Figure S3. Blood counts, Hemoglobin and Platelets determination. Blood specimens were collected 6 d and 20 d after the first dose of treatment. No significant changes in the blood counts were observed between treatment groups. At Day 6, compared to the control group of white blood cell (WBC) count of 7.19k/ μ l, the WBC count of PTUPB, cisplatin and the combination treatment were 7.94k/ μ l ($p = 0.889$), 3.69k/ μ l ($p = 0.426$) and 3.23k/ μ l ($p = 0.376$), respectively. At day 20, compared to the control group of white blood cell (WBC) count of 28.57k/ μ l, the WBC count of PTUPB, cisplatin and the combination treatment were 12.96 k/ μ l ($p = 0.337$), 3.25k/ μ l ($p = 0.394$) and 2.63k/ μ l ($p = 0.387$) . Because of large individual variations, we did not see any statistical significance. As an alkylating agent, cisplatin seemed to decrease WBC count, but addition of PTUPB to cisplatin did not further decrease WBC count. We did not observe any statistically significant difference of hemoglobin and platelet count among these four groups.

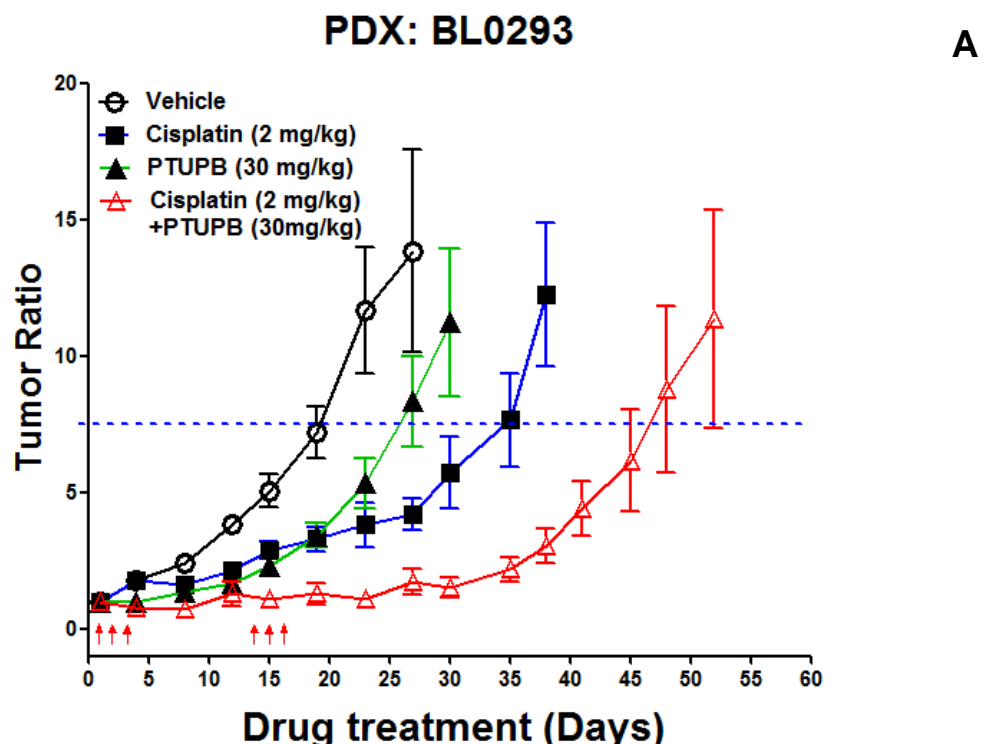
Figure S4. Biochemistry panel. Blood specimens were collected 6 d and 20 d after the first dose of treatment. No significant damage to liver and kidney in any of these groups as demonstrated in the liver function of aspartate transaminase (AST) and total bilirubin, and in the kidney function of blood urea nitrogen (BUN) and creatinine. AST: aspartate transaminase; BUN: alanine transaminase.

Figure S5. Histopathological evaluation of major organs (H&E staining). Cisplatin treatment induced old hemorrhage in the spleen red pulp characterized with focal hemosiderin deposit. The control and PTUPB treatment show no overt histological changes in the spleen red pulp and white pulp architecture. Cisplatin or combined treatment induced cytoplasmic vacuolization (microvesicular steatosis) in the hepatocytes that could be due to normal variations. There is minimal steatosis, mild portal, and lobular inflammation. No overt liver histologic changes were observed. No overt histological damage in the kidney tissue was detected in the control and PTUPB treatment groups. Cisplatin induced distal tubule cells swollen in the combined treatment. No overt histological damage in the heart tissues was caused by cisplatin treatment. These data demonstrated the safety application of COX-2/sEH dual inhibitor PTUPB plus cisplatin therapy in bladder cancer treatment.

Figure S6. IHC staining of bladder PDX tumor tissues (BL0293). Left panel: Comparison of morphology between the control and PTUPB groups in BL0293 PDX model. Hematoxylin and eosin stain (H & E stain) showed that more tumor cells in control group compared to the PTUPB plus Cisplatin-treated mice. Similarly, more Ki67 positive cells

were observed in the control group (middle panel), suggesting more cells were in cell proliferation. Right Panel: Staining of Cleaved Caspase 3. Compared with the control group, increasing numbers of cells stained positive for active caspase-3 in the PTUPB plus Cisplatin group indicating the progression of apoptosis across the cell population.

Figure 1



B

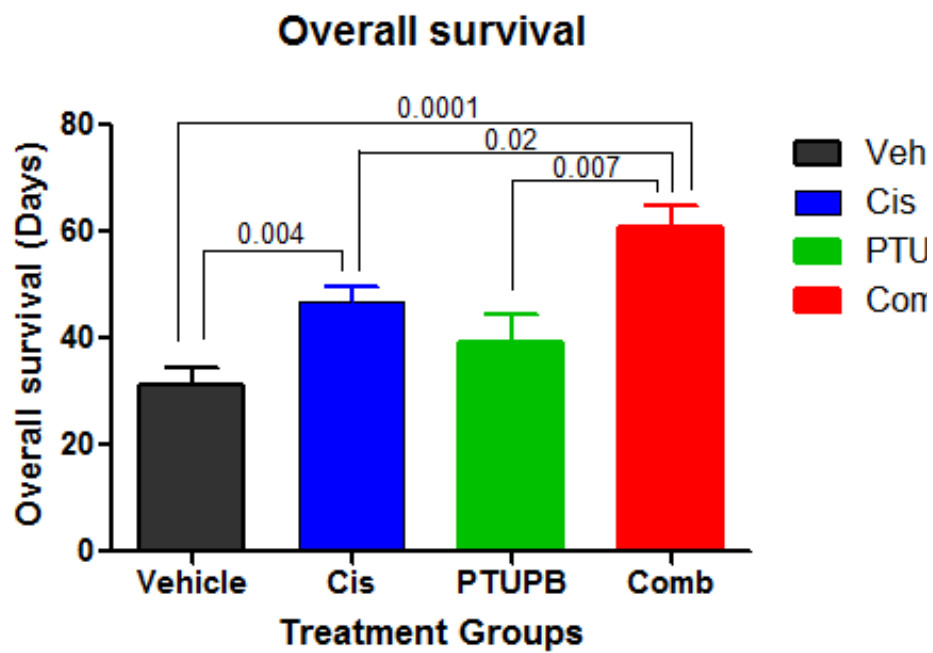


Figure 2

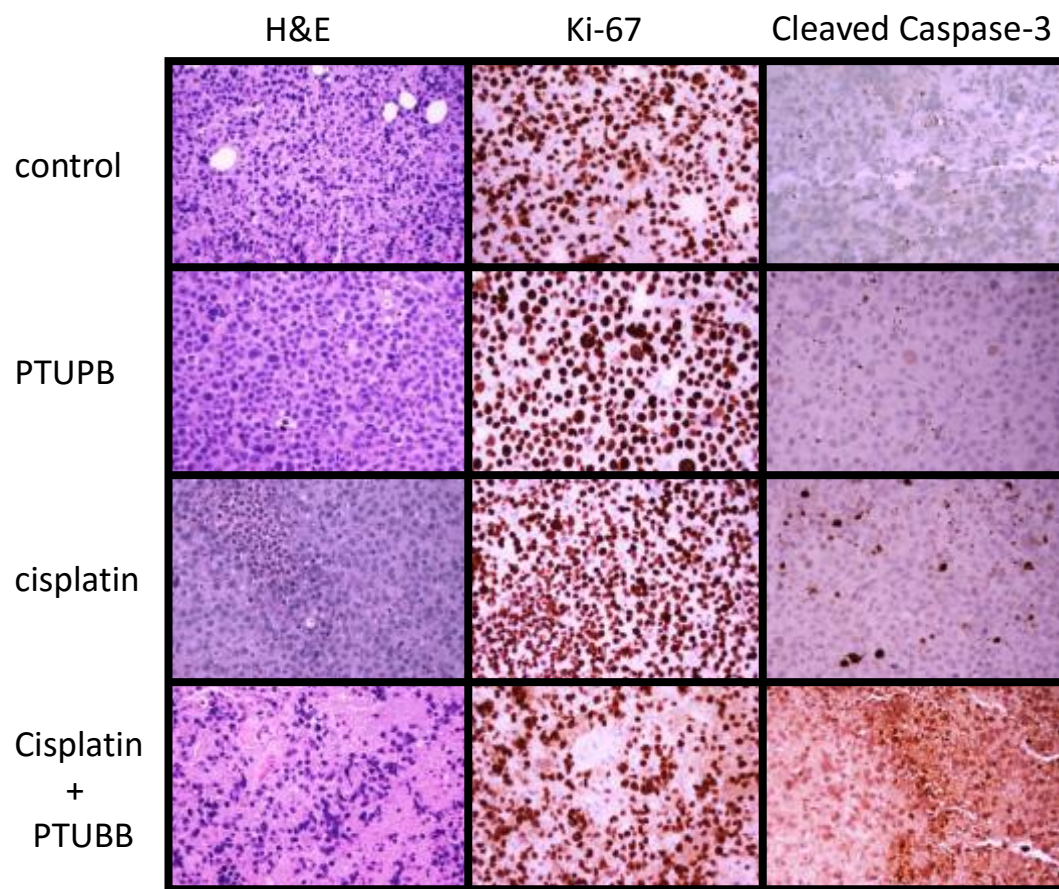


Figure 3

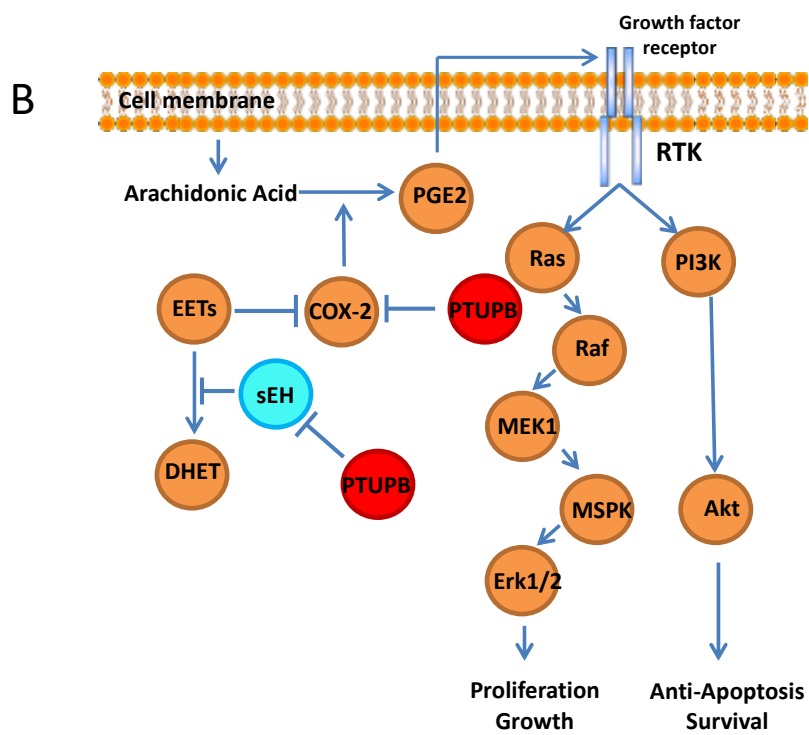
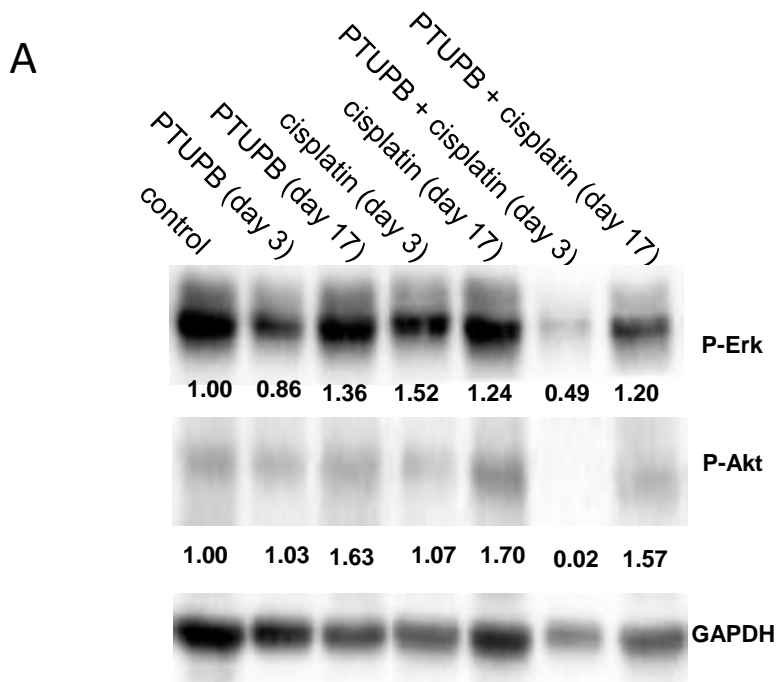
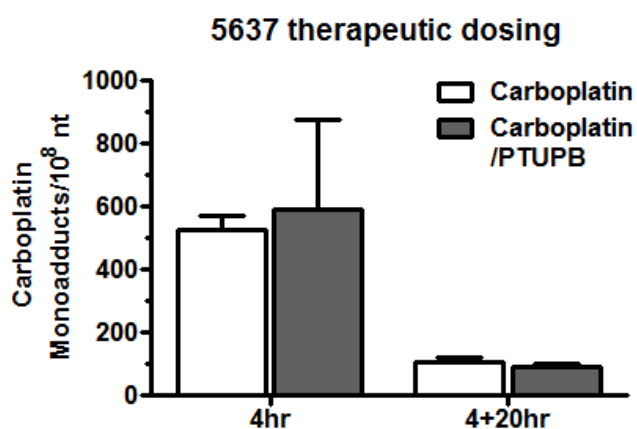
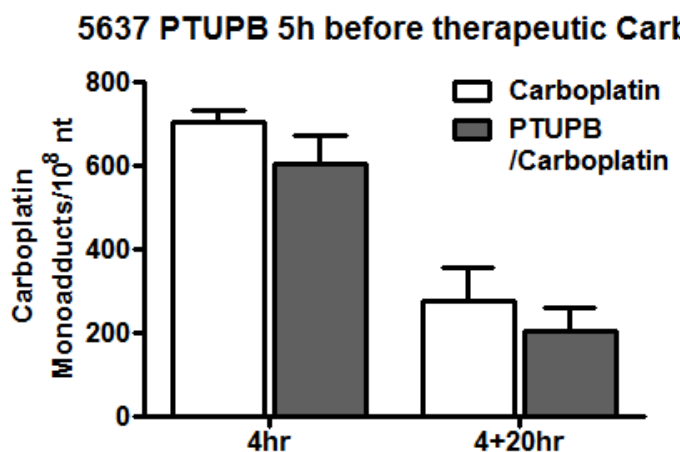


Figure 4

A



B



C

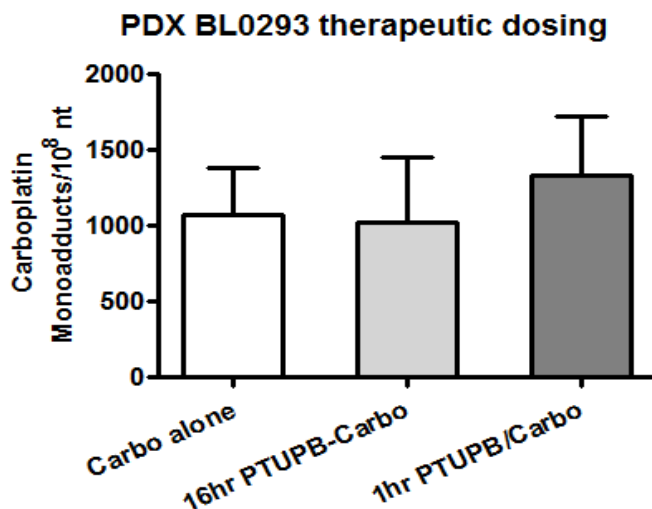
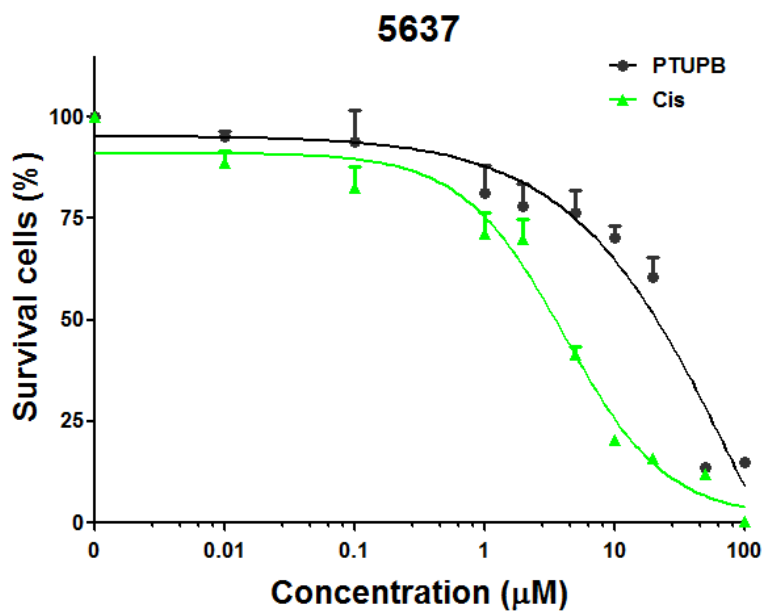
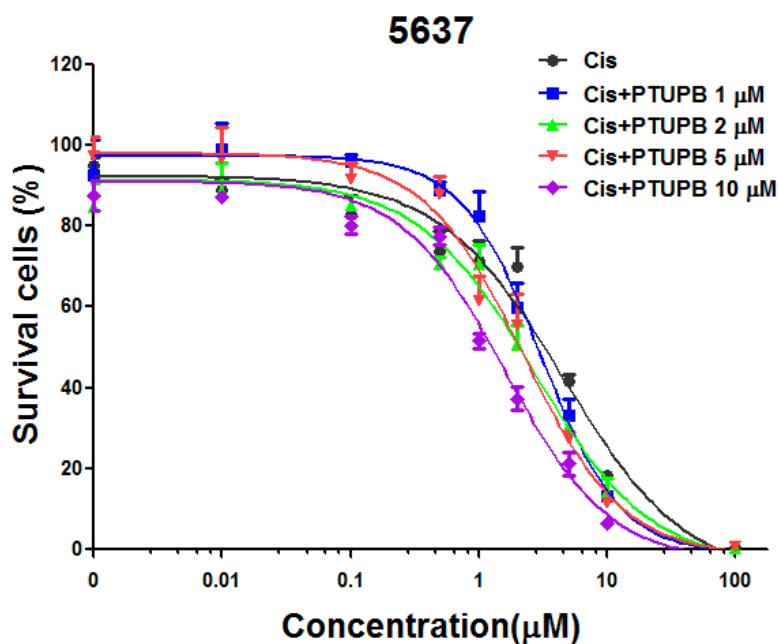


Figure 5

A



B

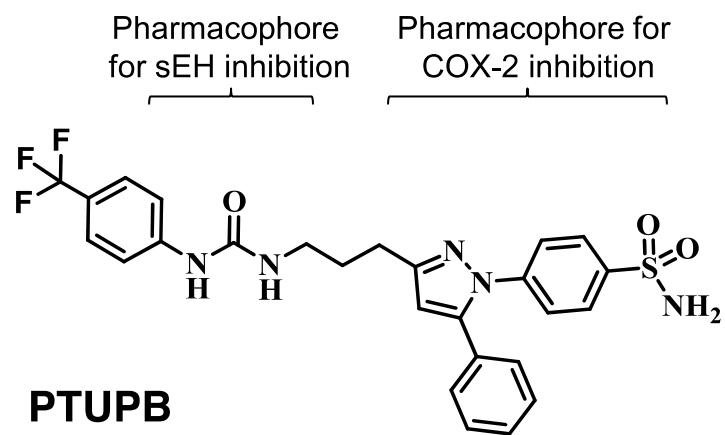


CI for Cisplatin+PTUPB

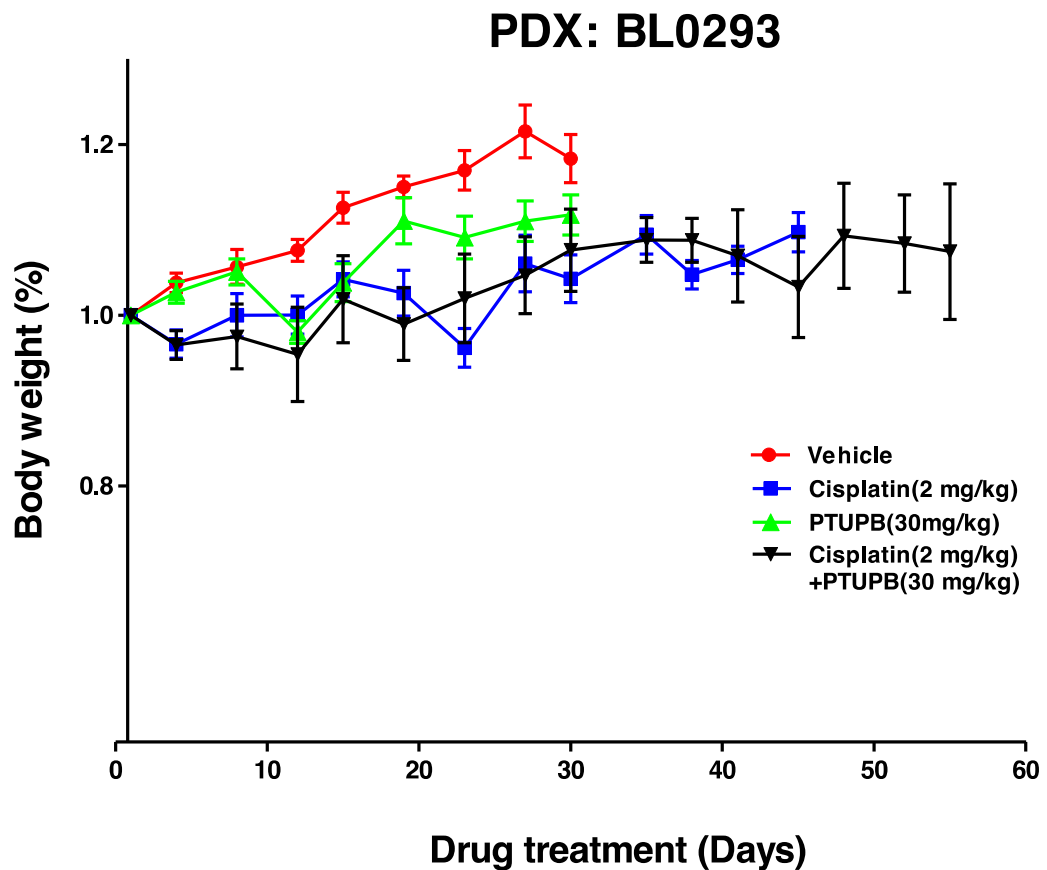
Cis(µM)	PTUPB(µM)	Effect	CI
5	1	0.33	0.94747
10	1	0.13	0.14292
5	2	0.30	0.79177
10	2	0.14	0.18015
5	5	0.27	0.76141
10	5	0.11	0.11442
5	10	0.21	0.50985
10	10	0.06	0.03263

Table 1. Drug-drug interaction between PTUPB and Cisplatin. Combination index values at different concentrations of PTUPB and cisplatin in 5637 bladder cancer cells.

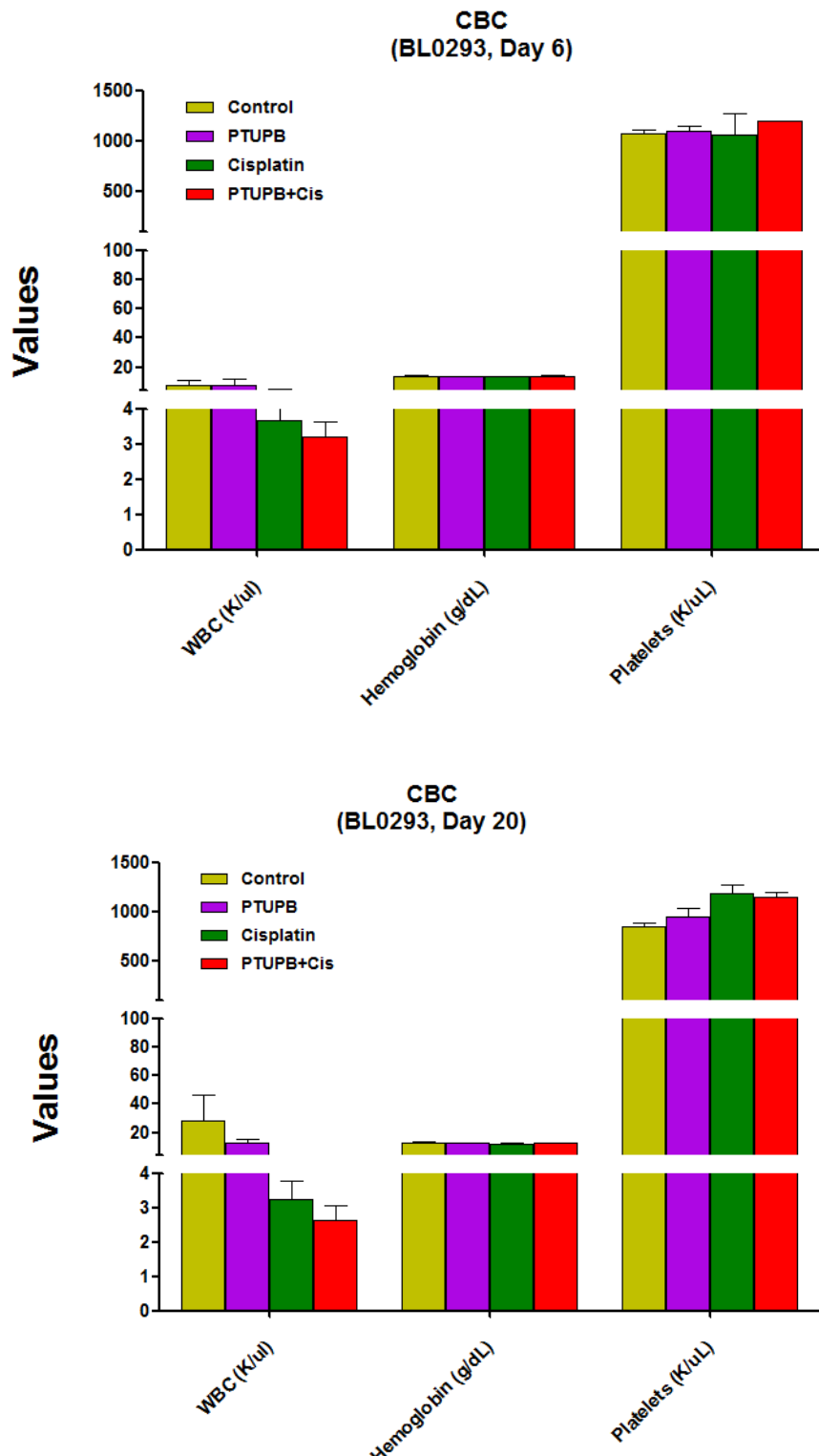
SI-Figure S1



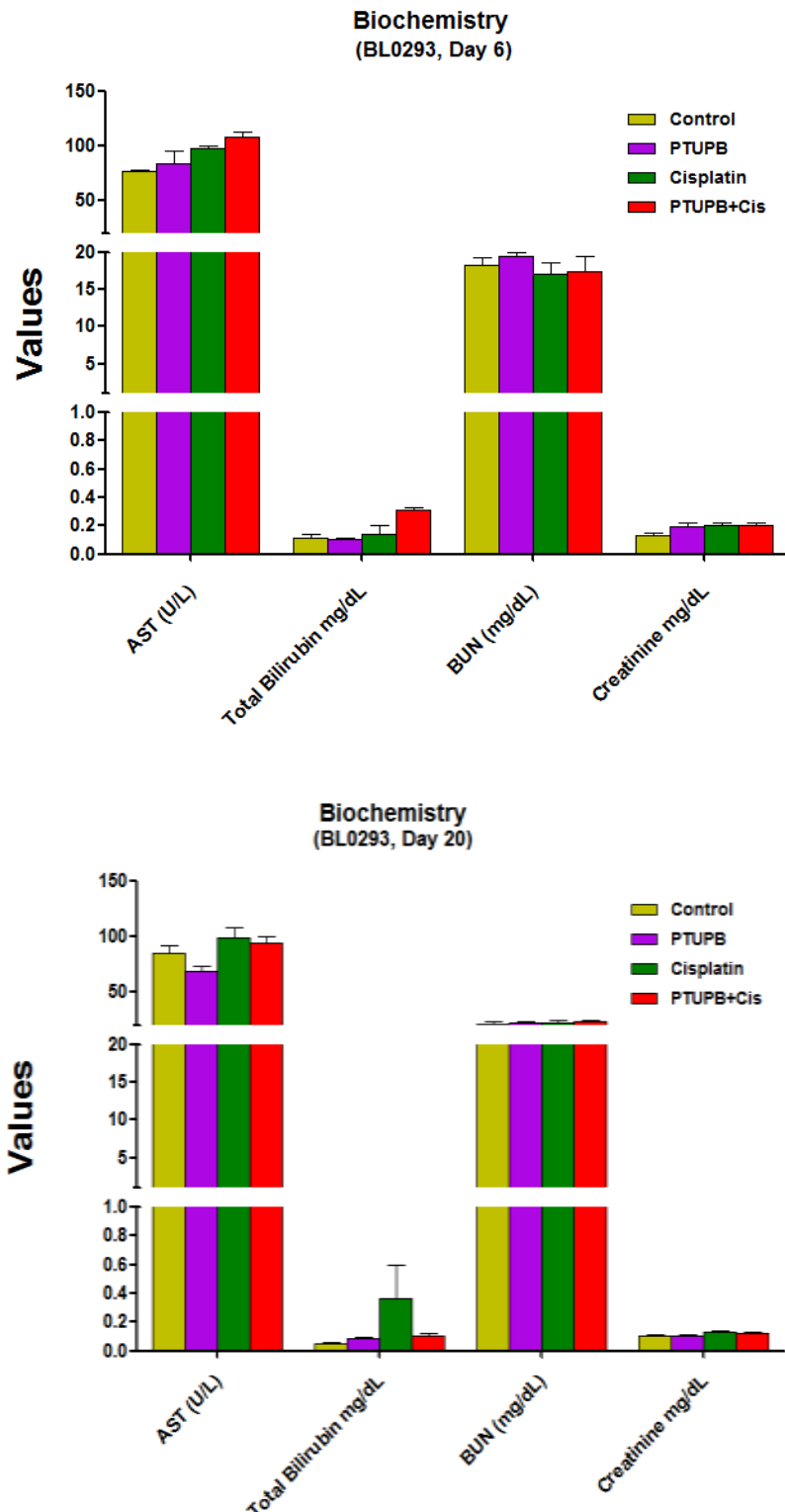
SI-Figure S2



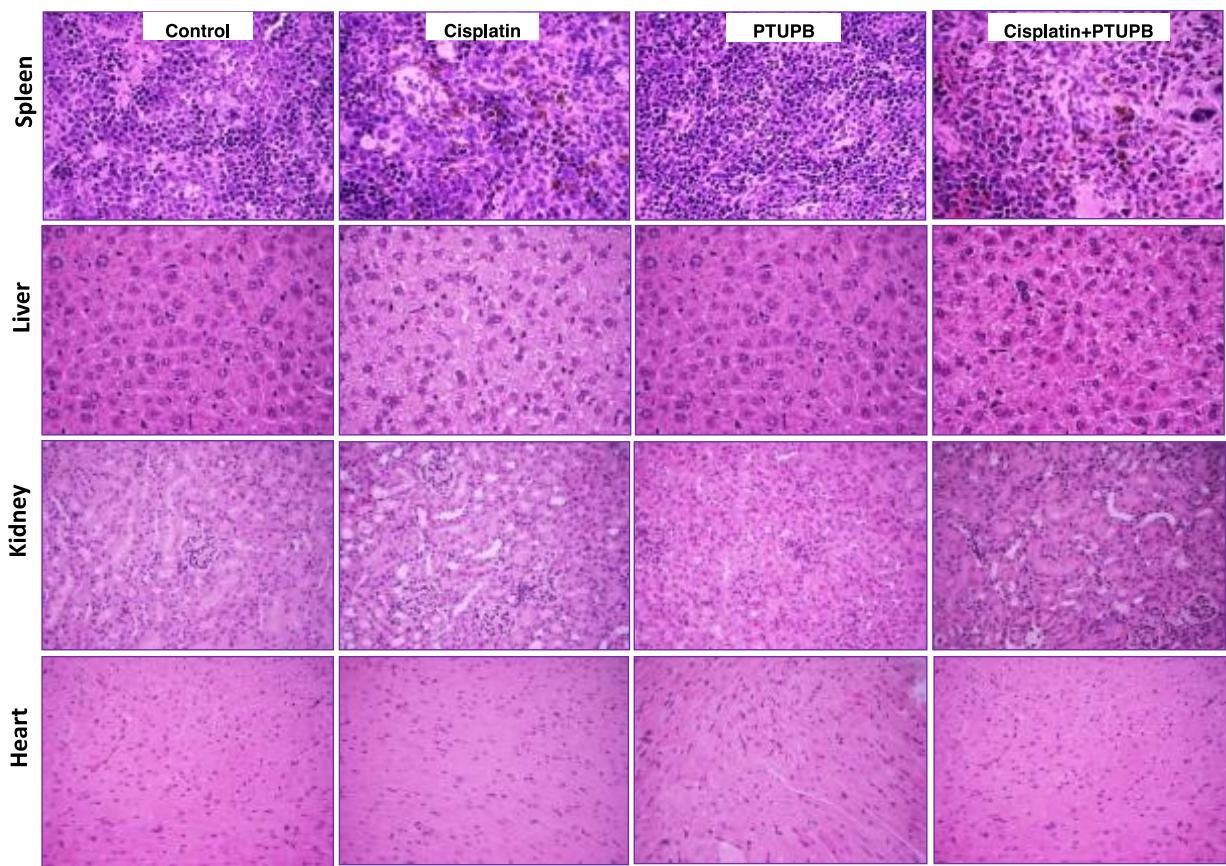
SI-Figure S3



SI-Figure S4



SI-Figure S5



SI-Figure S6

